Various RF Substrate Solutions for 22 nm FD-SOI Technology Targeting Cryogenic Applications

Martin Vanbrabant, Martin Rack, Dimitri Lederer, Valeriya Kilchytska, Jean-Pierre Raskin
Université catholique de Louvain, Belgium
martin.vanbrabant@uclouvain.be

***Abstract*—In this work, RF performance of standard and various high-resistivity (HR) substrates, namely including PN passivated ones, are evaluated at both room and cryogenic temperatures via the small-signal measurements of different passive elements, i.e. CPW and TFMS lines. The effective resistivity and the propagation losses of transmission lines are extracted. Degradation of substrates losses and an improvement of metallic losses at low temperature are shown. Finally, the PN interface passivation solution is evaluated for the first time to the authors' best knowledge, at cryogenic temperature and an improvement of effective resistivity by at least a factor 7x is observed over the HR substrate without any passivation solution.**

***Keywords*—CPW lines, cryogenic temperatures, FD-SOI, high-resistivity, parasitic surface conduction, PN interface passivation.**

I. Introduction

Nowadays, silicon CMOS technology and its advanced nodes are offering competitive performance for radio-frequency (RF) and millimeter-wave (mm-wave) applications. Recent CMOS technologies such as fully depleted silicon-on-insulator (FD-SOI) typically offer active devices featuring cutoff frequency (f_t) and maximum oscillation frequency (f_{max}) in the 300-400 GHz range [1]. Additionally, the rich back-end-of-line (BEOL) options [2] as well as the electromagnetic properties of the substrate highly contribute to the quality factor of mm-wave passive elements (i.e. inductors and capacitors) and interconnects. The silicon substrate can thus be responsible for significant losses, coupling and non-linearities if its resistivity is low [3]. Moving from standard resistivity substrates (with nominal resistivity ρ_{nom} = ~10 Ωcm) to high-resistivity (HR) substrates (ρ_{nom} > 1 kΩcm) helps mitigate these effects, though the improvements are hindered by the parasitic surface conduction (PSC) effect [4]. This effect originates from the formation of a thin highly conductive layer of free electrons attracted by the positive fixed oxide charges at the Si/SiO_2 interface [4], [5], resulting in a degradation of effective resistivity ρ_{eff} sensed by the coplanar circuitry on top of the silicon substrate [6].

In order to counter the PSC layer, several interface passivation solutions have been developed. In partially-depleted silicon-on-insulator (PD-SOI) technology, the trap-rich (TR) is a well-known solution which renders the interface resistive by introducing a thin layer of polysilicon underneath the buried oxide [5]. In FD-SOI technology, a compatible passivation solution is the PN passivation technique, which relies on the implant of alternating regions of P and N-type dopants. The previously conductive interface now becomes a series combination of low resistivity (N- and P-doped) and high resistivity (depletion junction) regions, resulting in an increase of the effective resistivity [7], [8]. In particular, strong improvements in substrate-induced losses and non-linearities of CPW lines as well as highly improved quality factor of RF inductors were demonstrated [9], [10].

Nowadays, cryogenic operation of electronic components and systems attracts a lot of attention mainly motivated by space [11] and quantum applications [12]. Characterization of both active and passive elements in these extreme conditions is thus crucial for circuit design [13] at cryogenic temperatures. In previous works, the impact of low temperature was studied on CPW lines on HR substrate [14], on inductors fabricated on standard, HR and TR substrates [15] and on metal-oxide-metal (MoM) capacitors, transformers, and resonators [16].

In this paper, the impact of cryogenic temperature on the propagation losses of transmission lines is investigated on substrates with various resistivities. On-wafer RF measurements of two types of CPW and one TFMS test structures were performed at both room and liquid nitrogen temperatures. The effectiveness of PN interface passivation solution at liquid nitrogen temperature is evaluated for the first time to the authors' best knowledge.

II. Fabricated Structures and Measurement Setup

Several transmission lines were designed and fabricated on the 22FDX® technology's back-end-of-line from GlobalFoundries on wafers with various substrate resistivities.

A. Line Geometries

Two types of CPW lines and one TFMS line are designed to have close 50 Ω of characteristic impedance Z_c as represented in Fig. 1. Each line is 760 µm long and accompanied by dedicated Open and Thru structures. The first CPW structure (LL CPW) is formed in stacked lower-level (LL) metal layers and has a signal line width W of 20 µm, and a signal to ground spacing S of 20 µm. The second CPW structure (TM CPW) is implemented in upper and thicker metal (TM) layers using W = 35 µm and S = 25 µm. Additionally, a TFMS line is designed with a 10 µm wide signal line implemented in the same thick metal layer as TM CPW and a ground plane in the medium thick metal layers stacked.

2024 IEEE/MTT-S International Microwave Symposium - IMS 2024 | 979-8-3503-7504-6/24/$31.00 ©2024 IEEE | DOI: 10.1109/IMS40175.2024.10600309

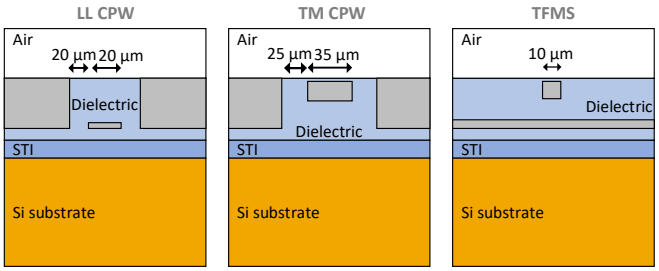

Fig. 1. Schematic cross-sections with main dimensions of the fabricated and characterized lines: LL and TM CPW lines and TFMS line.

B. Substrate Variants

Each structure is replicated on 4 wafers of different substrate resistivities as represented in Fig.2: (a) the process of reference (POR) on standard-resistivity (~10 Ωcm) wafer labelled as Std-POR, (b) another standard-resistivity (~10 Ωcm) wafer optimized for less conductive interface labelled as Std-Enh (PSC effect is still present), (c) a high-resistivity (985 Ωcm) wafer also optimized for less conductive interface labelled as HR-Enh and (d) that same HR-Enh substrate with PN-lines interface passivation. These PN junctions serve to increase the impedance between the signal and ground lines of the CPW by impeding the E-field path between these with multiple highly-resistive depletion regions. Through on-chip high-valued resistor elements, they can also be reverse biased in order to widen the depletion regions and further increase the substrate's interface impedance.

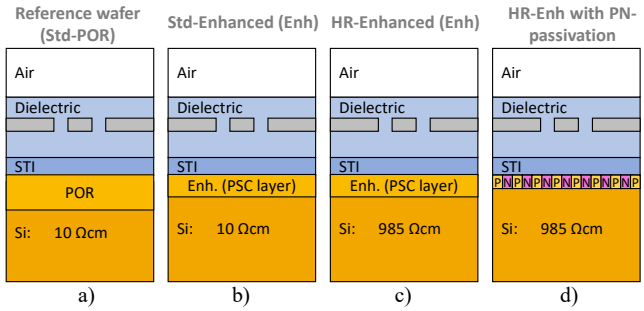

Fig. 2. Schematic cross-sections of the studied substrate variants: (a) Std-POR, (b) Std-Enh, (c) HR-Enh and (d) HR-Enh with PN-passivation.

C. Measurement Setup

S-parameters of the different transmission lines were measured using a pair of ground-signal-ground (GSG) Picoprobe® probes from 100 kHz to 40 GHz with a Keysight PNA N5291A vector network analyser (VNA). Both room temperature (295 K) and liquid nitrogen temperature (77 K) measurements were performed in a LakeShore CPX cryogenic probe station.

III. RF Performance Results

The transmission line measurements are first corrected by a Line-Reflect-Reflect-Match (LRRM) calibration at each temperature. From the S-parameters data, the effective resistivity ρ_{eff} of the underlying material and line loss α are extracted [17] after a Line-Line deembedding.

A. LL CPW Lines

The RF performance results obtained from the LL CPW lines on different substrates at 77 K and 295 K are shown in Fig. 3. As expected, at 295 K the effective resistivity of the standard resistivity substrates reach ρ_{eff}(20 GHz) = 8 and 13 Ωcm for Std-POR and Std-Enh, respectively. By moving to the high-resistivity substrate (HR-Enh), ρ_{eff}(20 GHz) goes up to 53 Ωcm which is way below its nominal resistivity value (985 Ωcm) because it suffers from PSC effect. As represented in Fig. 3.b, this translates into a 2.5 dB/mm (1.5 dB/mm) reduction in lineic loss at 20 GHz by moving from Std-POR (Std-Enh) to HR-Enh.

At 77 K, all substrates see a decrease of effective resistivity compared to their room temperature counterpart. This is due to the increase of carrier mobility at low temperature [18]. Std-POR and HR-Enh substrates demonstrate a decrease of ρ_{eff}(20 GHz) from 8 and 53 Ωcm at 295 K to 1.5 and 37 Ωcm, respectively. Interestingly, the lineic loss α(20 GHz) at 77 K increases for both standard resistivity substrates (+ ~6.5 dB/mm) but decreases for HR-Enh substrate (-0.3 dB/mm). The reason is that although all substrates suffer from ρ_{eff} decrease (substrate losses), the metallic losses are lower at 77 K. Therefore, in HR-Enh substrate, the improvement in metallic losses from temperature reduction outperforms the higher substrates losses, which is not the case for standard resistivity substrates, since losses are dominated by substrate losses rather than metallic ones.

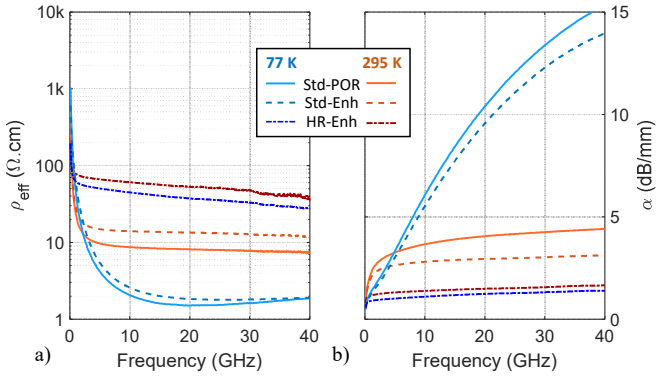

Fig. 3. Effective resistivity (a) and propagation losses (b) extracted from LL CPW lines on different substrates (Std-POR, Std-Enh and HR-Enh) at 77 K and 295 K.

Previous research [7] already demonstrated the efficiency of the PN interface passivation solution at room temperature. In Fig. 4, it can be seen that this solution stays beneficial at 77 K. Indeed, the effective resistivity (taken at 20 GHz) increases to 150 Ωcm at 295 K and 250 Ωcm at 77 K, when the PN passivation is present without any applied junction voltage. When applying a 3 V reverse PN bias, it enlarges the depletion regions of the PN junctions [19] and thus, ρ_{eff}(20 GHz) increases further to 350 Ωcm at 295 K and 510 Ωcm at 77 K. The propagation losses at V_{NP} = 3 V improve accordingly, with 0.39 dB/mm (at 295 K) and 0.63 dB/mm (at 77 K) improvement compared to the HR-Enh substrate without passivation.

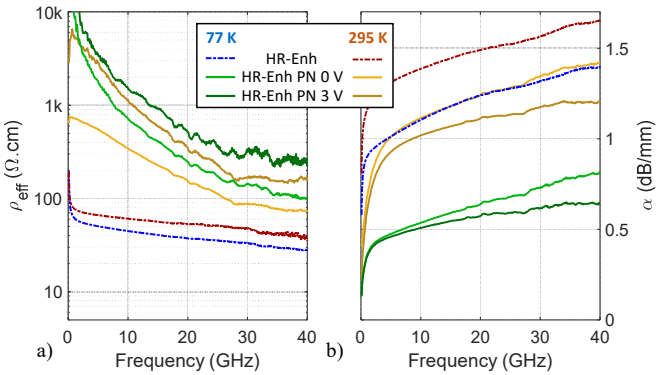

Fig. 4. Effective resistivity (a) and propagation losses (b) extracted from LL CPW line on HR-Enh with and without PN-passivation at 77 K and 295 K.

In Fig. 5, one can notice that PN passivation is more effective and thus ρ_{eff} is higher at low temperature (700 % improvement by moving from HR-Enh to HR-Enh PN 3V at 77 K compared to 230 % at 295 K), contrarily to all the other substrate cases. This is because of the depletion regions widening with temperature reduction (and thus acts just like the reverse PN bias).

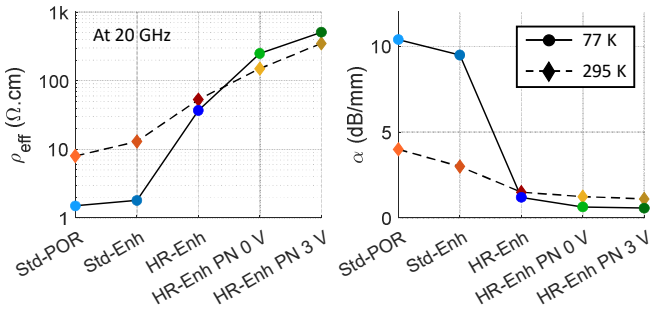

Fig. 5. Effective resistivity ρ_{eff}(20 GHz) and propagation losses α(20 GHz) extracted from LL CPW line on different substrates at 77 K and 295 K.

B. TM CPW and TFMS Lines

Similar benchmarking was performed on the TM CPW lines on different substrates at 77 K and 295 K as shown in Fig. 6. Along with the TM CPW propagation losses, the TFMS propagation losses are added for comparison.

Due to the larger distance between the CPW line and the substrate, the effective resistivity of TM CPW lines is larger compared to the values obtained from LL CPW lines. At room temperature, ρ_{eff} at 20 GHz increases from 44 Ωcm and 55 Ωcm for Std-POR/Enh substrates to 230 Ωcm for HR-Enh substrate. At 77 K, the extracted effective resistivity of all substrates above ~20 GHz is lower than at room temperature, similarly to LL CPW lines. It is also interesting to note that while ρ_{eff}(20 GHz) for HR-Enh decreases from 230 Ωcm at 295 K to 170 Ωcm at 77 K, the lineic loss at that same frequency is the same (Fig. 6.b), the change in the metallic and substrates losses perfectly compensating each other.

As represented in Fig. 6.b, the TFMS line demonstrates a 0.11 dB/mm improvement in α at 20 GHz by changing temperature from 295 K to 77 K. This can be mainly attributed to the improvement of metallic losses because of the shielding ground plane preventing any substrate losses.

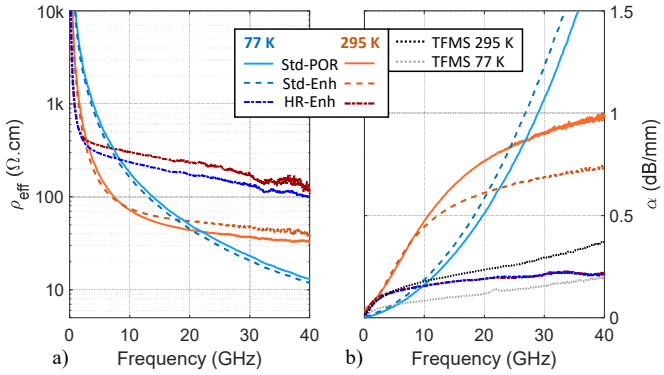

Fig. 6. Effective resistivity (a) and propagation losses (b) extracted from TM CPW lines on different substrates (Std-POR, Std-Enh and HR-Enh) at 77 K and 295 K. Propagation losses of a TFMS line added for comparison.

Similarly to LL CPW lines, TM CPW lines implemented on HR-Enh substrate greatly benefit from the PN passivation solution as shown in the effective resistivity (Fig. 7.a) and propagation losses (Fig. 7.b).

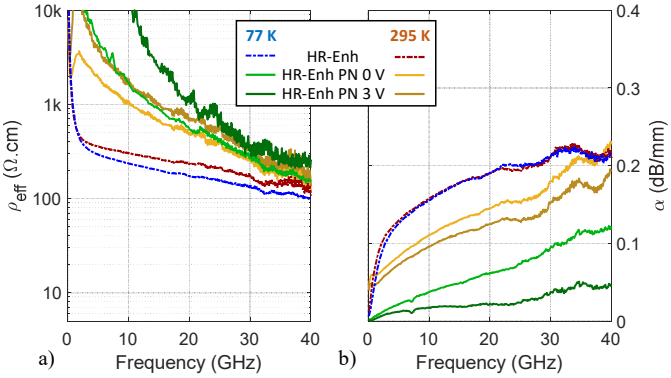

Fig. 7. Effective resistivity (a) and propagation losses (b) extracted from TM CPW line on HR-Enh with and without PN-passivation at 77 K and 295 K.

All RF metrics (extracted at 20 GHz) of the studied transmission lines are recapped in Table 1.

Table 1. RF FoMs of CPW and TFMS lines on different substrate options at 77 K and 295 K.

FoMs @ 20 GHz Line and substrate options.		**295 K**		**77 K**	
		α (dB/mm)	ρ_{eff} (Ωcm)	α (dB/mm)	ρ_{eff} (Ωcm)
LL CPW	Std-POR	4	8	10.4	1.5
	Std-Enh	3	13	9.5	1.8
	HR-Enh	1.5	53	1.2	37
	HR-Enh PN 0 V	1.24	150	0.64	250
	HR-Enh PN 3 V	1.11	350	0.57	510
TM CPW	Std-POR	0.76	44	0.51	50
	Std-Enh	0.61	55	0.58	45
	HR-Enh	0.19	230	0.19	170
	HR-Enh PN 0 V	0.15	490	0.06	550
	HR-Enh PN 3 V	0.13	700	0.02	1200
TFMS	All substrates	0.23	/	0.12	/

IV. Conclusion

In this paper, the RF performance of standard and high-resistivity substrates are assessed at both room and cryogenic temperatures via the measurements of several passive structures, i.e. CPW and TFMS lines.

At cryogenic temperature, the total propagation losses can be either higher or lower than at room temperature depending on the line geometry (particularly distance from the substrate) as well as the dominant contribution being either the metallic or substrate losses. Indeed, metallic losses decreases with temperature as clearly seen for TFMS line where an improvement of 0.11 dB/mm in α is measured at 20 GHz.

For substrates without the PN interface passivation (Std-POR, Std-Enh and HR-Enh), it is observed that a degradation in effective resistivity occurs when moving to liquid nitrogen temperature. However, contrarily to all the other substrate cases, HR-Enh PN substrate is more efficient at low temperature as the effective resistivity (at 20 GHz) increases by at least a factor 7x (PN 3 V) compared to HR-Enh substrate without passivation. Due to PN depletion junction widths increasing at lower temperatures, the PN-passivated substrates present improved RF performance at low temperature, especially under strong reverse bias conditions. Overall, the PN interface passivation solution offers excellent substrate figures of merit which stay true down to cryogenic temperature.

Acknowledgment

The authors would like to thank GlobalFoundries for chip fabrication and research support. This work is partially supported by the Fonds de la Recherche Scientifique (Belgium), via FNRS-PDR project “Cross-coupled effects in nanometer-scale transistors towards reliable cryogenic CMOS-based circuits” and by EC and Innoviris (Belgium – Brussels Region) via ECSEL JU “BEYOND5” project (grant agreement No 876124).

References

[1] R. Carter *et al.*, ‘22nm FDSOI technology for emerging mobile, Internet-of-Things, and RF applications’, in *2016 IEEE International Electron Devices Meeting (IEDM)*, Dec. 2016, p. 2.2.1-2.2.4. doi: 10.1109/IEDM.2016.7838029.

[2] S. N. Ong *et al.*, ‘A 22nm FDSOI Technology Optimized for RF/mmWave Applications’, in *2018 IEEE Radio Frequency Integrated Circuits Symposium (RFIC)*, Philadelphia, PA: IEEE, Jun. 2018, pp. 72–75. doi: 10.1109/RFIC.2018.8429035.

[3] J.-P. Raskin, ‘Fully Depleted SOI Technology for Millimeter-Wave Integrated Circuits’, *IEEE J. Electron Devices Soc.*, vol. 10, pp. 424–434, 2022, doi: 10.1109/JEDS.2022.3165877.

[4] Yunhong Wu, S. Gamble, B. M. Armstrong, V. F. Fusco, and J. A. C. Stewart, ‘SiO/sub 2/ interface layer effects on microwave loss of high-resistivity CPW line’, *IEEE Microw. Guid. Wave Lett.*, vol. 9, no. 1, pp. 10–12, Jan. 1999, doi: 10.1109/75.752108.

[5] M. Rack, F. Allibert, and J.-P. Raskin, ‘Modeling of Semiconductor Substrates for RF Applications: Part I—Static and Dynamic Physics of Carriers and Traps’, *IEEE Trans. Electron Devices*, vol. 68, no. 9, pp. 4598–4605, Sep. 2021, doi: 10.1109/TED.2021.3096777.

[6] M. Rack and J.-P. Raskin, ‘*(Invited)* SOI Technologies for RF and Millimeter Wave Applications’, *ECS Trans.*, vol. 92, no. 4, pp. 79–94, Jul. 2019, doi: 10.1149/09204.0079ecst.

[7] M. Rack, L. Nyssens, and J.-P. Raskin, ‘Low-Loss Si-Substrates Enhanced Using Buried PN Junctions for RF Applications’, *IEEE Electron Device Lett.*, vol. 40, no. 5, pp. 690–693, May 2019, doi: 10.1109/LED.2019.2908259.

[8] L. Nyssens *et al.*, ‘High-resistivity with PN interface passivation in 22 nm FD-SOI technology for low-loss passives at RF and millimeter-wave frequencies’, *Solid-State Electron.*, vol. 205, p. 108656, Jul. 2023, doi: 10.1016/j.sse.2023.108656.

[9] M. Rack, L. Nyssens, M. Nabet, D. Lederer, and J.-P. Raskin, ‘Impact of a High-resistivity Substrate on RF and mm-wave Performance of 22 nm FD-SOI Devices and Circuits’, in *Technologies Enabling Future Mobile Connectivity & Sensing*, River Publishers, 2023.

[10] M. Rack, L. Nyssens, and J.-P. Raskin, ‘Silicon-substrate enhancement technique enabling high quality integrated RF passives’, in *2019 IEEE MTT-S International Microwave Symposium (IMS)*, Boston, MA, USA: IEEE, Jun. 2019, pp. 1295–1298. doi: 10.1109/MWSYM.2019.8701095.

[11] L. Patterson, ‘Development of Electronics for Low-Temperature Space Missions’, 2001.

[12] M. Mehrpoo *et al.*, ‘Benefits and Challenges of Designing Cryogenic CMOS RF Circuits for Quantum Computers’, in *2019 IEEE International Symposium on Circuits and Systems (ISCAS)*, May 2019, pp. 1–5. doi: 10.1109/ISCAS.2019.8702452.

[13] A. Caglar and M. B. Yelten, ‘Design of Cryogenic LNAs for High Linearity in Space Applications’, *IEEE Trans. Circuits Syst. Regul. Pap.*, vol. 66, no. 12, pp. 4619–4627, Dec. 2019, doi: 10.1109/TCSI.2019.2936506.

[14] S. R. Taub and P. Young, ‘Temperature dependent performance of coplanar waveguide (CPW) on substrates of various materials’, in *1994 IEEE MTT-S International Microwave Symposium Digest (Cat. No.94CH3389-4)*, San Diego, CA, USA: IEEE, 1994, pp. 1049–1051. doi: 10.1109/MWSYM.1994.335175.

[15] Q. Berlingard *et al.*, ‘RF performance of Standard, High-Resistivity and Trap-Rich Silicon substrates down to cryogenic temperature’, in *ESSDERC 2023 - IEEE 53rd European Solid-State Device Research Conference (ESSDERC)*, Lisbon, Portugal: IEEE, Sep. 2023, pp. 148–151. doi: 10.1109/ESSDERC59256.2023.10268536.

[16] B. Patra, M. Mehrpoo, A. Ruffino, F. Sebastiano, E. Charbon, and M. Babaie, ‘Characterization and Analysis of On-Chip Microwave Passive Components at Cryogenic Temperatures’, *IEEE J. Electron Devices Soc.*, vol. 8, pp. 448–456, 2020, doi: 10.1109/JEDS.2020.2986722.

[17] L. Nyssens, M. Rack, and J.-P. Raskin, ‘Effective resistivity extraction of low-loss silicon substrates at millimeter-wave frequencies’, *Int. J. Microw. Wirel. Technol.*, vol. 12, no. 7, pp. 615–628, Sep. 2020, doi: 10.1017/S175907872000077X.

[18] S. M. Sze and K. K. Ng, *Physics of Semiconductor Devices*, 1st ed. Wiley, 2006. doi: 10.1002/0470068329.

[19] K. K. Nanda and S. N. Sarangi, ‘Electrical properties of 1N4007 silicon diode’, *Rev. Sci. Instrum.*, vol. 68, no. 7, pp. 2904–2908, Jul. 1997, doi: 10.1063/1.1148215.